Experimental Damage Assessment of the Garisenda Tower Combining Measurements of Optical Fiber Strains, Pendulum Displacements, and Acoustic Emission

Experimental Damage Assessment of the Garisenda Tower combining Measurements of Optical Fiber Strains, Pendulum Displacements, and Acoustic Emission

Giuseppe Lacidogna[1], Pedro Marin Montanari[1], Stefano Invernizzi[1], Angelo Di Tommaso[3], and Alberto Carpinteri[1,4]

[1]Politecnico di Torino, Corso Duca degli Abruzzi, 24, 10129 Torino, Italy

[3]Alma Mater Studiorum Università di Bologna, 40126 Bologna, Italy

[4]Shantou University, 243 Daxue Road, Shantou, Guangdong, China

ABSTRACT

One of the most important medieval remnants and a municipal icon in Bologna (Italy) is the Garisenda Tower. It was built in the early 12th century at the same time as the Asinelli Tower. The towers, known as the "Due Torri" of Bologna, were initially intended to be the same height, but in 1351, the Garisenda started to tilt because of foundation subsidence. As a result, it was reduced in height from 61 m to around 13 m for safety, today sitting at 48 m (about half of the 97 m of the Asinelli). The Garisenda Tower is wide 7.5 m on its sides, with walls up to 2 m thick, and it leans about 3.22 m to the East side. Since the beginning of the last century the structural behavior of the tower has been studied and, in more recent years, the topic of the tower's stability started to gain traction. This sparked the interest of assessing structural damage and cracking evolution by means of different non-destructive testing (NDT) techniques. There is currently a multitude of sensors installed in the Garisenda Tower. More precisely, 16 Acoustic Emission (AE) sensors, six thermometers, five Fiber Optic Sensors (FOS), four extensometers, two accelerometers, one seismometer, and (impressively) a 30 m long pendulum are located inside the tower. The accelerometers and the thermometers are present in the Garisenda since 2009. The optical strands were installed on March 2019, and were followed by the AE sensors on May 2019. The pendulum was installed on March 2021 and, lastly, the extensometers on June 2021. Together, these instruments compose a database capable of analyzing and relating various aspects of the mechanical behavior of the tower: with the aid of the FOS, the extensometers, and the pendulum, the steady-state displacement regime of the tower can be described by means of displacements and strains. This data can be confronted with AE and temperature data to quantify damage, for example. Short term events, such as seismic activity, can also be analysed via AE and the seismometers. In these regards, the present work intends to showcase a methodology for the damage assessment of the Garisenda tower in Bologna by the combined analysis of some of these sensors. In particular, the pendulum displacements, the FOS strains, and AE data will be analysed. These highlight how the correlation of different SHM equipment datasets can provide valuable insights about the damage state of the tower (particularly by means of the b-value parameter), and the mechanical behavior – in particular, its in-plane movements.

Keywords: Structural Health Monitoring, masonry structures, Fiber Optical Strands, Acoustic Emission, *b*-value

INTRODUCTION

Structural health monitoring (SHM) of historic buildings, and particularly of masonry structures, has been a recurrent theme of interest in the scientific community due to the need for cultural heritage preservation [1-5]. Among the myriad of constructions of this type in Italy, the Garisenda tower, together with the neighboring Asinelli tower, is a particularly important one, being one of the most recognizable symbols of the city of Bologna [6] (see Fig 1). Both are equipped with various tools to continuously monitor their structural conditions [7-8]. Regarding the Garisenda, examples of monitoring devices installed include Fiber Optical Strings (FOS), piezoelectric Acoustic Emission (AE) sensors, wire extensometers, thermometers, accelerometers, seismometers, and even a 30 m long pendulum installed on the inside to measure the movement of the top. This rich in-situ setup has sparked investigation of the structural behavior and health assessment of the tower under different viewpoints. Using numerical and/or experimental data, aspects such as material degradation [9-10], earthquakes and dynamic events [11-14], seasonal effects [15], among others, have been studied. The present work aims to contribute to this discussion by showcasing how the pendulum displacements, together with the FOS strains, can be used to determine the evolution trend of the leaning of the tower, and how AE data can give insights on the damage level of the tower basement by means of *b*-value [16]. Further studies will focus on building a finite element model considering the "smeared crack" formulation to relate Acoustic Emission to crack development. The working principle of the SHM devices present in the Garisenda tower will be described in the following. The pendulum was installed in the tower in February 2021 to monitor the horizontal motion of the summit. The pendulum measurement system collects data automatically every six hours and transmits it to a data management program. It can measure movements up to 100 mm in the X direction (pointing southeast) and up to 50 mm in the Y direction (pointing northeast). The accuracy of these measurements is within 0.075% of the maximum reading or 0.075 mm for X and 0.0375 mm for Y. To monitor the deformation of the tower basement, as well as the internal temperature in this region, a monitoring system utilizing vertically arranged fiber optical strands, provided by the firm Osmos, was employed, together with a thermometer. The gathered data, captured at a rate of 100 Hz with a sensitivity of one micrometer, is forwarded to an advanced data acquisition unit (EDAS) for initial processing, brief storage, and transfer to a specialized cloud. The information can be retrieved and downloaded through a designated web portal. Regarding AE monitoring, two AE devices (AE001 and AE002) each featuring eight channels and connecting to eight piezoelectric sensors are currently installed in the tower basement. The AE001 device was installed on May 31, 2019, while the AE002 device was installed on March 14, 2023. The piezoelectric sensor network is designed for Acoustic Emission (AE) local damage detection, utilizing Lunitek AEmission model LT18 -003-PRD00-R0 sensors sensitive in a frequency range of 15-625 kHz. The system enables real-time signal analysis and parameter extraction from the PZT sensors, with a sampling rate of 5 MS/s at 16 bits. The PZT sensors are securely attached to the tower inner wall using high-strength glue, ensuring stable attachment even in harsh environments.

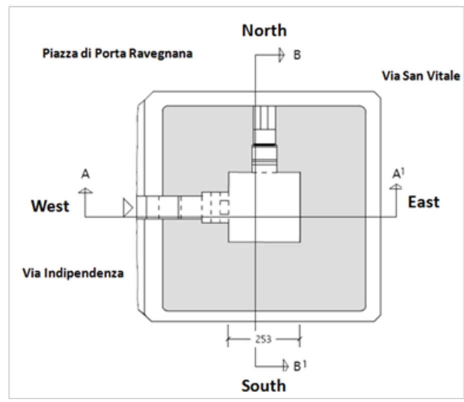

(a) (b)

Fig 1 The Asinelli and the Garisenda Towers in the city centre of Bologna (a), Garisenda tower basement level plan (b).

The basement masonry of the Garisenda tower has an overall thickness of about 275 cm and, starting from the inside of the cell, is composed of a depth of about 40 cm of selenite (a particular variety of crystalline gypsum) block masonry, a filling of heterogeneous "a sacco" masonry of about 150 cm, and about 80 cm of selenite blocks on the outside, including the ashlar coating

PENDULUM DISPLACEMENT, FOS STRAIN, AND AE *b*-VALUE ANALYSES

The pendulum and the FOS data were analysed together to determine the behavior of the in-plane movement of the tower. The mean pendulum position from February 2021 to May 2023 is shown in Fig 2a. The mean position of the pendulum in 2021 and in 2023 in the months of February, March, April, and May, is shown in Fig 2(b–e).

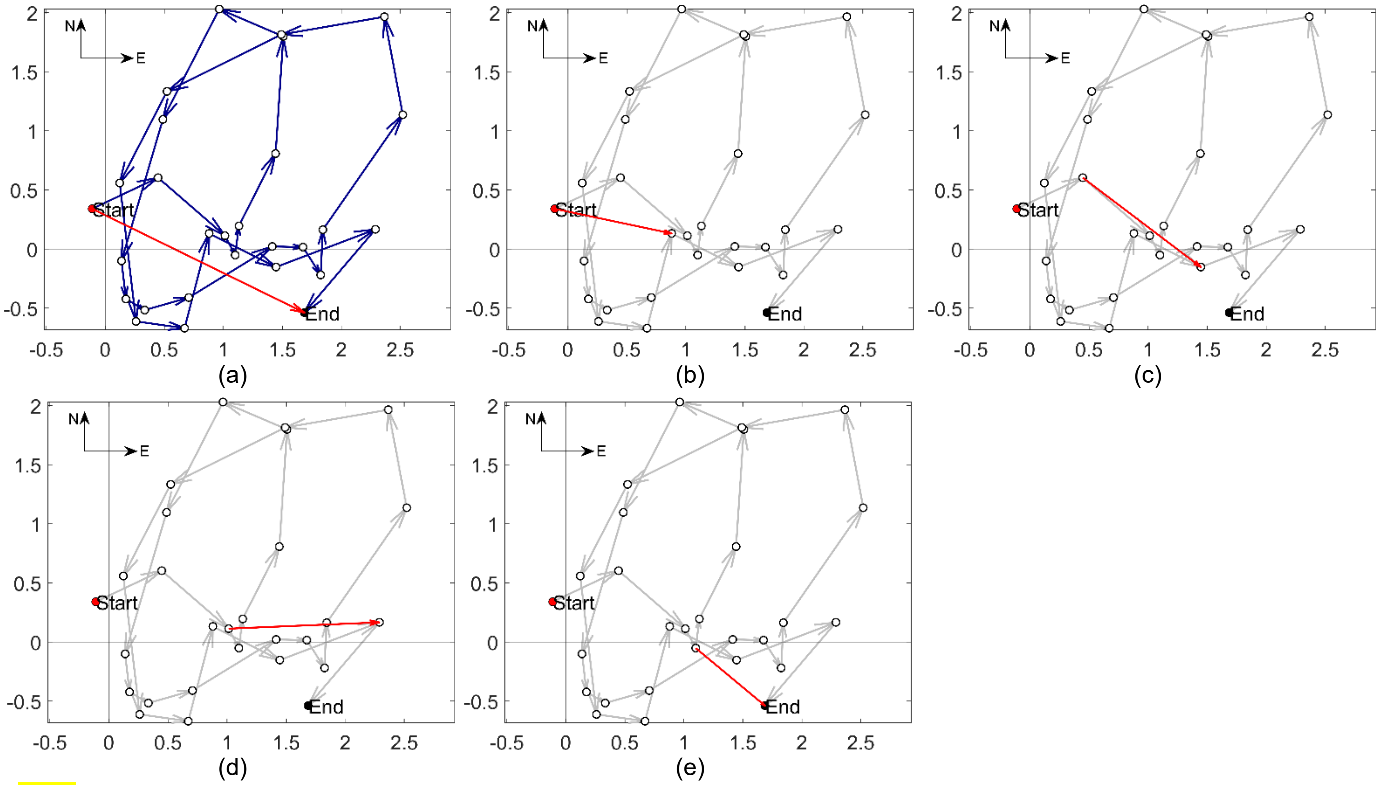

Fig 2 The mean monthly pendulum position from February 2021 to May 2023 (a), the mean position of the pendulum in 2021 and in 2023 in the months of February (b), March (c), April (d), and May (e)

Overall, the pendulum presented a tendency to move south-eastwards – which is the direction of leaning of the tower. In particular, the average monthly displacements of the pendulum from these analyses seems to be of around 0.9 mm southwards and 1.5 mm eastwards over the period of three years. The pendulum displacements in the X and Y directions were compared to the deformation tendency obtained by means of the FOSs O1_NW, O2_NE, and O3_SE. These three strings were chosen because they are arranged in the inner corners of the tower cell, as seen in Fig2a. The O4_SW optical string, although present in one of the corners, was not considered, as it stopped working in 2020. Fig 3a shows the disposition of the FOS in the basement of the tower. By calculating the differences between their deformations, it is possible to represent the orientation of the inclination of the tower basement and its vertical displacements. To carry out this analysis, the deformation of each string was represented in a 3D space, in which the origin of the reference system is in the center of gravity of the basement of the tower. The x and y coordinates of the strings are those of the inner edges of the tower cell, while the z coordinates represent the recorded deformation. Starting from these 3 vectors it is possible to define a plane in space, having angular coefficients "a" and "b" (measured in [m^{-1}]) in the x and y directions respectively, as reported in Fig 3b.

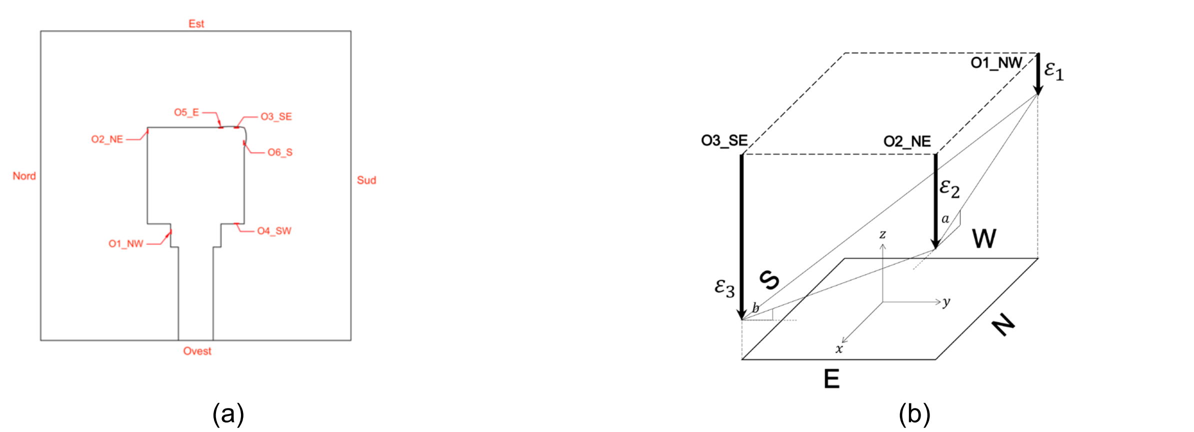

Fig 3 The disposition of the FOSs in the inner wall of the tower basement (a) and their deformation represented in the 3D space (b)

Considering the rest of the tower, beyond the basement, as a rigid body, these angular coefficients then represent the trends in the displacements of the top of the tower over time. Fig 4 shows the comparison between the hourly displacements recorded by the pendulum and the magnitude of the angular coefficients in the east-west direction (4a) and in the north-south direction (4b).

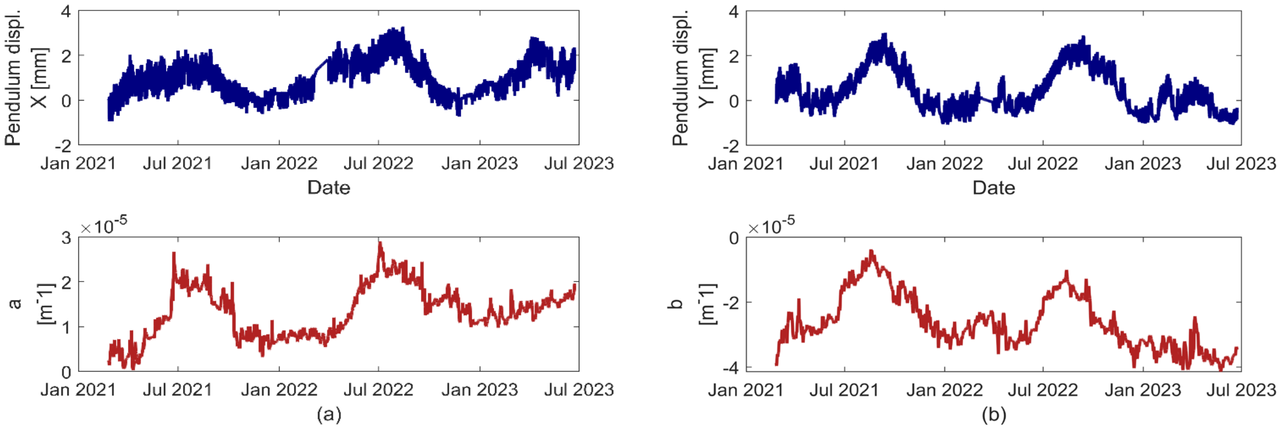

Fig 4 Comparison between the hourly displacements recorded by the pendulum and the magnitude of the angular coefficients in the east-west direction (a) and in the north-south direction (b)

The trends in the displacements of the top of the tower in the x and y directions are in phase with those obtained by the pendulum starting from February 25, 2021, the date of its installation. The displacements recorded by the pendulum and the strains recorded by the FOS present a cyclic component and a trend component. These components were separated for the pendulum displacements and for the FOS strains. To do this, the "detrend" function of the MATLAB program was used. This function subtracts the best-fit line of a data series (in case of a linear trend). In the case of the pendulum, the periodic cyclic part could correspond to displacements due to daily and seasonal temperature variations, that are recoverable and are in fact periodically retrieved, and can be seen in Fig 5.

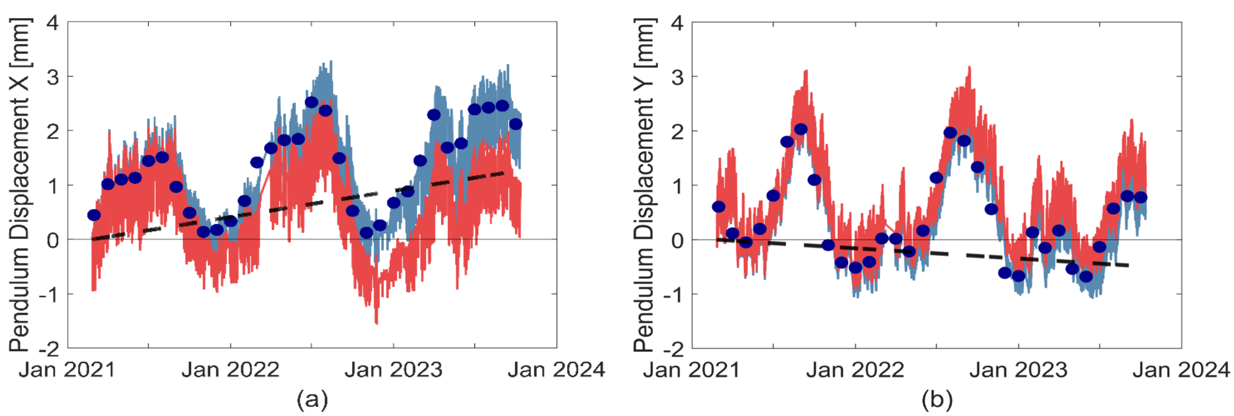

Fig 5 Periodic and trend components of the pendulum displacements on the east-west direction (a) and on the north-south direction (b). The blue curve is the original signal, the red curve is the periodic component (the detrended signal) and the black dashed line is the trend. The blue scatter corresponds to the mean pendulum displacements in the x and y directions and are the same points depicted in Fig 2a

The permanent part, on the other hand, could correspond to displacements generated by the creep phenomenon, i.e. the deformations under constant load of the tower basement produced by the action of the tower dead load. Considering the monitoring period of about three years, the total displacements calculated using this approach are of around 1.5 mm eastward and 0.6 mm southward, which is comparable to the ones found by calculating the evolution of the mean monthly pendulum position presented in Fig 2a. The calculation of the FOS strains trend was also carried out and presented in Fig 6. This was done by first considering the individual strain of each string, Fig 6(a–e), and then the average strain of the five optical strings, Fig 6f. In analogy with the case of the pendulum, the strain measured by the five strings can be separated into periodic and a permanent parts.

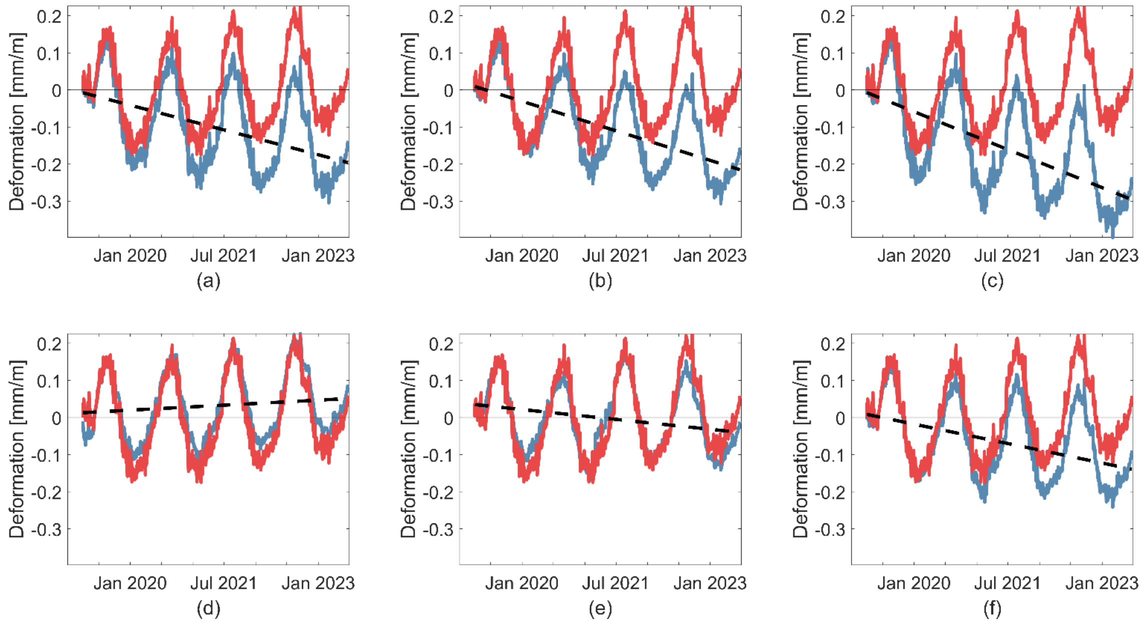

Fig 6 Periodic and trend component of the FOS strains: O1_NW (a), O2_NE (b), O3_SE (c), O5_E (d), O6_S (e) and mean value of all strands (f). The blue curve is the original signal, the red curve is the periodic component (the detrended part) and the black dashed line is the trend

Almost all optical strings strains show a clear downward trend. The only exception is the O5_E string (installed on the inner wall to the east). That string, rather than shortening, tends to deform positively, which represents an elongation. Evidently, it can be said that the behavior of the O5_E string is anomalous: on one hand because all the other strings have an inverse behavior, on the other hand, because the string, having a length of about 1 m, is shorter than the others (2 m long) and for this reason it could capture a local behavior along the masonry axis e on which it is applied. Based on the previous discussion, only the O1_NW, O2_NE and O3_SE optical strings were taken into consideration. The lowering tendency evidenced by the optical strings is congruent with the movements of the pendulum. Also, from this analysis the FOS that shows the greatest contractions is the O3_SE, followed in order by the O2_NE and the O1_NW. This observation is congruent with the one obtained through the determination of the angular coefficients. The FOS deformations were also analysed together with the accumulated number of AE signals. From this, an interesting pattern can be identified. The increasing rate in the generation of AE signals seem to coincide with the lowest values of deformation – that is, the maximum contraction of the FOS - which occur in cold periods, as can be seen in Fig 7.

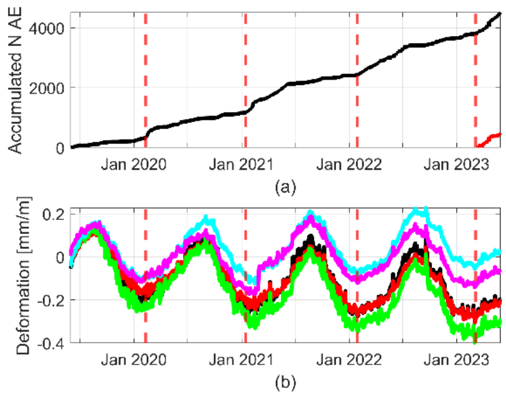

Fig 7 Accumulated number of AE signals (a) in correspondence to the deformation of the FOS (b). In (a) the black line corresponds to data from AE001 and the red line from AE002. In (b) the deformations of the strings O1_NW, O2_NE, O3_SE. O5_E and O6_S are represented respectively in black, red, lime, cyan, and magenta. The vertical dotted red lines on the graph indicate the coldest periods during the monitoring period, which typically correspond to a higher rate of generated AE signals.

The higher rate of generation of AE signals in these cold periods could indicate that the basement of the Garisenda tower experiences greater damaging on cold periods than on hot periods. To verify if that is the case, a *b*-value analysis was carried out, using the data from the AE sensors located in the basement of the tower. A schematic of the disposition of the sensors is indicated in Fig 8.

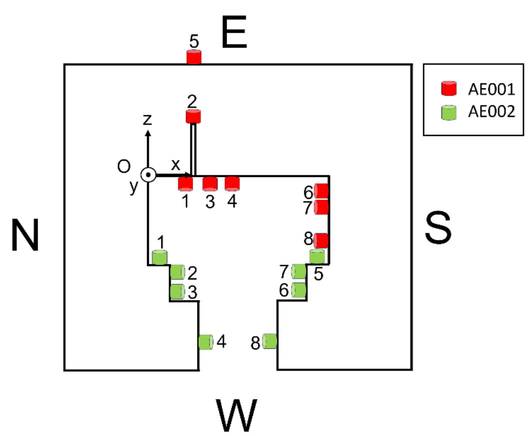

Fig 8 Disposition of the AE sensors in the tower basement

In fracture mechanics, the *b*-value corresponds to a fractal measure of damage. Values closer to 1.5 correspond to fractures distributed throughout a volume, whereas values closer to unity are representative of nucleation of cracks on a fracture surface, which indicates a particularly dangerous situation [17-18]. To assess the damage effects in hot periods and in cold periods, two *b*-value analyses were conducted. The 1st period considered AE signals from January 30, 2022, to August 13, 2022. This was considered the onset towards the hot period of the year, as it starts in the winter and ends in summer. The 2nd period considered AE signals from August 14, 2022, to March 3, 2023. This was considered the onset towards the cold period of the year, as it starts in the summer and ends in winter. Only signals from the equipment AE001, with a frequency "f" in kHz in the range $50 \leq f \leq 400$ and an amplitude "A" in mV in the range $2 \geq A \geq 0.7$, were considered. The *b*-value was calculated based on the daily average amplitude of all the detected AE signals [19]. A sliding window scheme was used with a width of 10 signals and a step of two signal – that is, the *b*-value of the 1st window corresponds to the calculations performed with signals 1–10, then for the 2nd window with signals 8–17, and so on. Fig 9 presents the *b*-value together with the amplitude of the AE signals and the accumulated number of AE signals. The green dashed line corresponds to a *b*-value of 1.5 (critical condition), while the red one corresponds to 1.0 (forming cracks condition).

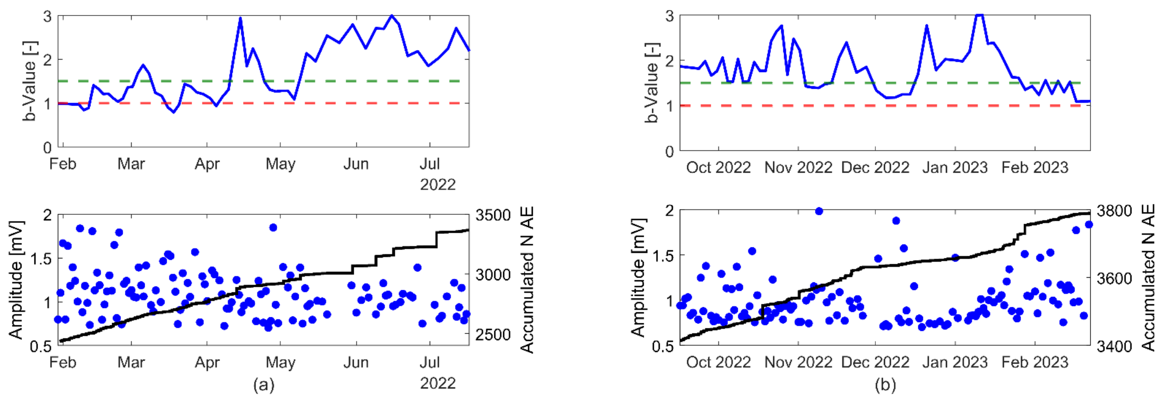

Fig 9 *b*-value (top), amplitudes of the AE signals (bottom, blue scatter), and accumulated number of signals (bottom, black curve) in the onset towards the hot period (a), and in the onset towards the cold period (b)

In the onset towards the hot period (Fig 9a) the *b*-value starts low and ends high, and it seems to present a trend to increase throughout. This indicates a likelihood of damage decreasing as temperatures rise. That is, crack nucleation has the tendency to shift from forming cracks surfaces conditions (*b*-value ~ 1.0) to more uniformly distributed microcracks throughout the material of the tower basement. In the onset towards the cold period (Fig 9b), the *b*-value starts high and ends low, and seems to present a trend to decrease throughout. This indicates a likelihood of damage increasing as temperatures fall. In this case crack nucleation shifts from distributed microcracks to the coalescence of crack surfaces. The proximity of the *b*-value to values close to unity during colder periods is also associated, as it was assessed previously, with the higher rate of generation of AE signals. This results in a greater distribution of high amplitude signals, which contributes to reducing the *b*-value approaching 1.0. The current *b*-value analyses, along with this observation, suggest that the damage of the tower basement is more pronounced during colder periods compared to warmer ones.

CONCLUSIONS

In this contribution, analyses of different monitoring devices installed in the Garisenda tower have been performed to give insights on its mechanical behavior and its damage evolution. The analysis of the pendulum displacements and of the FOS strains highlighted a similar behavior. The strains of the FOS were in phase with the pendulum displacements. Both the pendulum displacements and the FOS strains could be separated into periodic and trend components. The periodic component represents the recoverable part of the motion. This could be due, for example, to seasonal effects such as temperature. The trend component represents the non-recoverable part of the motion. This could be associated to damage. The trends of both the pendulum displacements and of the FOS strains indicated a tendency of movement of the top of the tower towards south-east (which is the direction of the leaning). This tendency of movement was valued as 1.5 mm to the east and 0.6 mm to the south in three years. The FOS strains were also analysed together with the accumulated number of AE signals. It could be seen that the peak of generation of AE events seemed to coincide with the maximum contraction of the FOS, which occurred in cold periods. To further understand the damage during hot and cold periods, a *b*-value analysis was conducted using AE data from the tower basement sensors. The analysis showed a trend of increasing *b*-values from January to August 2022 (hot period onset) and decreasing *b*-values from August 2022 to March 2023 (cold period onset). This indicates that damage is more severe during cold periods compared to hot periods.

ACKNOWLEDGEMENTS

The authors acknowledge the Municipality of Bologna for allowing the publication of this study, and thank the companies R Teknos S.r.l., OSMOS ITALIA s.r.l., and Tecno In S.p.A. for their support and data.

REFERENCES

[1] B. Simonetta, P. Michele, S. Silvestri, G. Gasparini, and T. Trombetti, SSHM and DSHM for a better knowledge and risk prevention of historical buildings: The cases of the Two Towers in Bologna and the Cathedral in Modena, in: IEEE Workshop on Environmental, Energy, and Structural Monitoring Systems (EESMS) Proceedings, Trento, Italy: IEEE, pp. 180–185 (2015). doi:10.1109/EESMS.2015.7175874.

[2] A. Carpinteri, S. Invernizzi, and G. Lacidogna, In situ damage assessment and nonlinear modelling of a historical masonry tower, Engineering Structures, vol. 27, n. 3, pp. 387–395 (2005). doi:10.1016/j.engstruct.2004.11.001.
[3] A. Anzani, L. Binda, A. Carpinteri, S. Invernizzi, and G. Lacidogna, A multilevel approach for the damage assessment of Historic masonry towers, Journal of Cultural Heritage, vol. 11, n. 4, pp. 459–470 (2010). doi:10.1016/j.culher.2009.11.008.
[4] R. M. Azzara, M. Girardi, V. Iafolla, C. Padovani, and D. Pellegrini, Long-term dynamic monitoring of medieval masonry towers, Front. Built Environ, vol. 6, pp. 1–15, Art. 9 (2020). doi:10.3389/fbuil.2020.00009.
[5] A. Carpinteri, G. Lacidogna, and N. Pugno, Structural damage diagnosis and life-time assessment by acoustic emission monitoring, Engineering Fracture Mechanics vol. 74, n. 1–2, pp. 273–289 (2007). doi:10.1016/j.engfracmech.2006.01.036.
[6] F. Giordano "La Torre Garisenda", Costa Ed. Bologna, 2000 (In Italian).
[7] S. Baraccani, M. Palermo, G. Gasparini, and T. Trombetti, A time domain approach for data interpretation from long-term static monitoring of historical structures, Struct Control Health Monit vol. 28 (2021). doi:10.1002/stc.2708.
[8] S. Baraccani, M. Palermo, S. Silvestri, G. Gasparini, T. Trombetti, and R. M. Azzara, The static and dynamic monitoring of the Asinelli Tower in Bologna, Italy, presented at the 8th European Workshop On Structural Health Monitoring (EWSHM 2016), Bilbao, Spain: NDT.net (2016). Available: https://www.ndt.net/events/EWSHM2016/app/content/Paper/287_Baraccani_Rev2.pdf
[9] S. Baraccani, A. Piccolo, G. Gasparini, M. Palermo, and T. Trombetti, An assessment of the structural behaviour of the Garisenda tower in Bologna through finite element modelling and structural health monitoring. Proceedings of the 7th International Conference on Computational Methods in Structural Dynamics and Earthquake Engineering (COMPDYN 2015), pp. 5416–5422 (2019). doi:10.7712/120119.7314.19061.
[10] G. Dallavalle, A. Di Tommaso, G. Gottardi, T. Trombetti, R. Lancellotta, and S. Lugli, “The Garisenda Tower in Bologna: Effects of degradation of selenite basement on its static behaviour.,” in Geotechnical Engineering for the Preservation of Monuments and Historic Sites III, 1st ed., London: CRC Press, 2022, pp. 1088–1100. doi: 10.1201/9781003308867-86.
[11] R. M. Azzara, A. Cavaliere, S. Danesi, A. Morelli, and L. Zaccarelli, Il monitoraggio sismico della Torre degli Asinelli e della Garisenda. Risultati preliminari dell’analisi dei dati (2014). doi: 10.13140/RG.2.1.3378.5443.
[12] S. Baraccani, R. M. Azzara, G. Gasparini, A. Morelli, M. Palermo, T. Trombetti, L. Zaccarelli, Identification through seismometric measurements of transients propagating inside the Asinelli and Garisenda towers (Bologna, Italy), implication on structural modeling and state of health monitoring, in Proceedings of the 7th International Conference on Computational Methods in Structural Dynamics and Earthquake Engineering (COMPDYN 2015), Crete, Greece: Institute of Structural Analysis and Antiseismic Research School of Civil Engineering National Technical University of Athens (NTUA) Greece, 2019, pp. 3881–3892. doi: 10.7712/120119.7193.19071.
[13] A. D. Tommaso, G. C. Olivetti, G. Lacidogna, O. Borla, S. Invernizzi, and A. Carpinteri, Garisenda Tower in Bologna (Italy): Health monitoring by different nondestructive testing techniques, IJMRI, vol. 9, n. 1–2, pp. 54-66 (2023). doi: 10.1504/IJMRI.2023.10053442.
[14] S. Baraccani, R. M. Azzara, M. Palermo, G. Gasparini, and T. Trombetti, Long-term seismometric monitoring of the two Towers of Bologna (Italy): Modal frequencies identification and effects due to traffic induced vibrations, Front. Built Environ. vol. 6, pp. 1-14, Art. 85 (2020). doi:10.3389/fbuil.2020.00085.
[15] A. D. Tommaso, G. C. Olivetti, G. Lacidogna, S. Invernizzi, and A. Carpinteri, Garisenda Tower in Bologna (Italy): Structural assessment and numerical simulation, IJMRI (2024) (In print). doi: 10.1504/IJMRI.2023.10053441.
[16] G. Lacidogna, G. Niccolini, and A. Carpinteri, Health Monitoring of Medieval Masonry Towers by an Acoustic Emission Approach, KEM, vol. 817, pp. 586–593 (2019). doi:10.4028/www.scientific.net/KEM.817.586.
[17] A. Carpinteri, G. Lacidogna, and S. Puzzi, From criticality to final collapse: Evolution of the ‘b-value’ from 1.5 to 1.0, Chaos, Solitons & Fractals, vol. 41, n. 2, pp. 843–853 (2009). doi:10.1016/j.chaos.2008.04.010.
[18] S. Colombo, I. G. Main, and M. C. Forde, Assessing damage of reinforced concrete beam using "b -value" analysis of acoustic emission signals, J. Mater. Civ. Eng. vol. 15, n. 3, pp. 280–286 (2003). 10.1061/(ASCE)0899-1561(2003)15:3(280)
[19] Q. Han, L. Wang, J. Xu, A. Carpinteri, and G. Lacidogna, A robust method to estimate the b-value of the magnitude–frequency distribution of earthquakes, Chaos, Solitons & Fractals, vol. 81, pp. 103–110 (2015). doi:10.1016/j.chaos.2015.09.004.